

January 13, 2022
 PREPARED FOR SUBMISSION TO JHEP

N³LO gravitational quadratic-in-spin interactions at G^4

Michèle Levi,^{a,b} Andrew J. McLeod,^a and Matthew von Hippel^a

^a*Niels Bohr International Academy, Niels Bohr Institute, University of Copenhagen,
 Blegdamsvej 17, 2100 Copenhagen, Denmark*

^b*Institut de Physique Théorique, CEA & CNRS, Université Paris-Saclay,
 91191 Gif-sur-Yvette, France*

E-mail: michelelevi@nbi.ku.dk, amcleod@nbi.ku.dk, mvonhippel@nbi.ku.dk

ABSTRACT: We compute the N³LO gravitational quadratic-in-spin interactions at G^4 in the post-Newtonian (PN) expansion via the effective field theory (EFT) of gravitating spinning objects for the first time. This result contributes at the 5PN order for maximally-spinning compact objects, adding the spinning case to the static sector at this PN accuracy. This sector requires extending the EFT of a spinning particle beyond linear order in the curvature to include higher-order operators quadratic in the curvature that are relevant at this PN order. We make use of a diagrammatic expansion in the worldline picture, and rely on our recent upgrade of the `EFTofPNG` code, which we further extend to handle this sector. Similar to the spin-orbit sector, we find that the contributing three-loop graphs give rise to divergences, logarithms, and transcendental numbers. However, in this sector all of these features conspire to cancel out from the final result, which contains only finite rational terms.

Contents

1	Introduction	1
2	EFT of gravitating spinning objects	3
2.1	Extending the EFT of a spinning particle	5
3	Perturbative expansion of quadratic-in-spin interactions	6
4	N³LO gravitational quadratic-in-spin action at G^4	8
5	Conclusions	9

1 Introduction

As of 2016 the observation of gravitational waves (GWs) has become a reality [1]. An unexpected variety of GW events has already been observed from black hole and neutron star binary mergers on the first and second observation runs of the LIGO and Virgo collaborations [2–4]. The continuously increasing influx of data expected from the expanding worldwide network of ground-based interferometers [5–8] and anticipated space-based detectors in complementary frequencies [9, 10] places significant demands on the precision of theoretical predictions. The theoretical waveform templates used for these observations are uniquely created using the effective one-body (EOB) framework [11, 12], which in turn relies heavily on the post-Newtonian (PN) theory of General Relativity as input [13]. Even relatively high-order corrections beyond Newtonian gravity, such as the sixth PN (6PN) order, are required for accurate waveforms, and to gain further information about the inner structure of the individual components of the binary.

PN theory provides an analytic treatment of the long inspiral phase, in which the two compact objects in the binary move with non-relativistic velocities. The orbital dynamics of the compact binaries is an essential ingredient for theoretical waveform models. The current state of the art for orbital dynamics for generic compact binaries in PN theory is presented in table 1. This table shows the sectors obtained at order $n + l + \text{Parity}(l)/2$ in the PN expansion, where l is the order of spin that appears in the sector with the corresponding parity for even or odd l , and for $l \geq 2$ finite-size effects have to be tackled. Along the years much of the progress in PN theory has been made only for the simple unrealistic case, in which the compact objects are not spinning and are considered as point-masses (corresponding to the first row in table 1), due to the considerable conceptual and computational difficulty of treating spinning objects in gravity.

Nevertheless, in recent years remarkable progress has also been made in the spinning sectors via the effective field theory (EFT) approach to PN gravity [14, 15] within the

$\begin{smallmatrix} n \\ l \end{smallmatrix}$	$(N^0)\text{LO}$	$N^{(1)}\text{LO}$	$N^2\text{LO}$	$N^3\text{LO}$	$N^4\text{LO}$	$N^5\text{LO}$
S^0	1	0	3	0	25	0
S^1	2	7	32	174		
S^2	2	2	18	52		
S^3	4	24				
S^4	3	5				

Table 1. The minimum number of n -loop graphs within the EFT framework for each PN sector that has been completed to date for the orbital dynamics of generic compact binaries. The gray area indicates the sectors that correspond to gravitational Compton scattering with quantum spins $s \geq 3/2$.

framework of the EFT of gravitating spinning objects [16]. The filled entries in table 1 show the number of n -loop graphs that contribute within the EFT framework in each $N^n\text{LO}$ sector that has been completed to date. The boldface entries in the table have been completed only via the EFT of gravitating spinning objects [16], in a series of works [17–26]. In particular, in [16] the leading non-minimal gravitational couplings to all orders in spin were formulated, thus enabling the completion of all sectors with finite-size effects up to the current state of the art at the 4PN order.

This line of work was recently extended along both of the axes of table 1: The first three-loop calculation in the spinning sector was computed in [25], using the publicly-available `EFTofPNG` code [23], and the cubic- and quartic-in-spin sectors were tackled at one-loop level in [24, 26]. The latter sectors thus uniquely explore the gray area in table 1, which corresponds to gravitational Compton scattering with quantum spins $s \geq 3/2$, as sectors with classical spin at the l -th order correspond to scattering with quantum spin of $s = l/2$ [27]. Altogether, this has been pushing the precision frontier to the 5PN order.

This work derives for the first time the complete $N^3\text{LO}$ gravitational interactions which are quadratic in the spins from a diagrammatic expansion at order G^4 . All contributions at this order are static, meaning that they involve no explicit factors of the velocities of the compact objects. This sector involves both three-loop graphs and finite-size effects due to the spin-induced quadrupole. It enters at the 5PN order for maximally-spinning compact objects, thus further pushing the precision frontier of PN gravity. This work builds on the EFT of gravitating spinning objects [16] and its implementation in the publicly-available `EFTofPNG` code in [23], as well as on their recent implementations and upgrade at the two-loop level [21] and at the three-loop level [25].

As noted above the spinning sectors are considerably more challenging to handle than the non-spinning ones. First, contrary to the non-spinning case, in the spinning sectors all possible graph topologies are realized at each order of G [28]. While there are no three-loop graphs that enter in the non-spinning $N^3\text{LO}$ sector, in the present sector there are 52 such graphs (see table 1), which turn out to be precisely those that produce divergences and logarithms. Further, this sector contains 163 graphs to evaluate compared to only

8 in the $N^3\text{LO}$ sector without spins. We also recall that spins are derivatively coupled, which in this sector with two spins leads to integrand tensor numerators up to rank eight, comparable to $N^5\text{LO}$ in the sector without spins. Finally, at this order we also have to consider further contributions from higher-order operators with spins that are beyond linear in the curvature (note, however, that tails that involve spin couplings do not contribute at the order considered here [13, 29]).

The paper is organized as follows. We begin in section 2 by reviewing the formal framework of the EFT of gravitating spinning objects, which we extend in section 2.1 to include further non-minimal couplings in the effective action of a spinning particle that become relevant at this order. We proceed in section 3 to consider the diagrammatic expansion of interactions that are quadratic in the spins, highlighting how the graphs in this sector can be constructed out of the graphs in lower-order sectors. We discuss the total outcome for the sector in section 4, and conclude in section 5.

2 EFT of gravitating spinning objects

We start by reviewing the framework of the EFT of gravitating spinning objects, which enables our derivation of the $N^3\text{LO}$ quadratic-in-spin sectors from a diagrammatic expansion at order G^4 . We follow closely the setup presented in the recent work [25] and also build on [21], keeping similar conventions and notations. First we will extend the one-particle effective action that was required for the $N^3\text{LO}$ spin-orbit in [25], introducing further Feynman rules that are required in this sector. Thus, from the two-particle effective action that describes a compact binary [14, 15]:

$$S_{\text{eff}} = S_g[g_{\mu\nu}] + \sum_{a=1}^2 S_{\text{pp}}(\lambda_a), \quad (2.1)$$

we will only be concerned with S_{pp} , the worldline action of a spinning particle for each of the two components of the binary, where λ_a are their respective worldline parameters.

From the pure gravitational action, S_g , given in [25] in the harmonic gauge, no additional ingredients are required beyond those presented in [25]. Hence, we use similar propagators for the gravitational field components in terms of the Kaluza-Klein (KK) decomposition [30, 31], and no further bulk vertices are required beyond those which were added in [25]. As in [25] the spatial dimension, d , is kept generic throughout, which also matches what is done in the `EFTofPNG` code [23]. We use the corresponding d -dimensional gravitational constant [25],

$$G_d \equiv G_N \left(\sqrt{4\pi e^\gamma} R_0 \right)^{d-3}, \quad (2.2)$$

where $G_N \equiv G$ is Newton's gravitational constant in three-dimensional space, γ is Euler's constant, and R_0 is a fixed renormalization scale. This corresponds to the modified minimal subtraction ($\overline{\text{MS}}$) prescription in dimensional regularization used in this work, see e.g. [32]. As in the $N^3\text{LO}$ sector at order G^4 in [25] relativistic corrections to the propagators are not relevant in this paper.

We now focus on the point-particle action for each of the spinning particles [15, 16]. The quadratic-in-spin sector includes three types of interaction: i. the coupling between the spins of both objects, referred to as the $\text{spin}_1\text{-spin}_2$ interaction, ii. the nonlinear interaction of each object's spin with itself, referred to as $\text{spin}_1\text{-spin}_1$ interaction, and iii. finite-size effects that involve the spin-induced quadrupole of each of the rotating objects. Due to the latter interaction, the effective action should be considered beyond minimal coupling, which is sufficient for the spin-orbit sector, and for interactions that are dependent on the linear spin couplings as in the $\text{spin}_1\text{-spin}_2$ and $\text{spin}_1\text{-spin}_1$ interactions. Considering all these interactions, the effective action of each of the spinning particles reads [15, 16]:

$$S_{\text{pp}}(\lambda) = \int d\lambda \left[-m\sqrt{u^2} - \frac{1}{2}\hat{S}_{\mu\nu}\hat{\Omega}^{\mu\nu} - \frac{\hat{S}^{\mu\nu}p_\nu}{p^2} \frac{Dp_\mu}{D\lambda} + L_{\text{NMC}}[g_{\mu\nu}, u^\mu, S^\mu] \right], \quad (2.3)$$

where L_{NMC} denotes the non-minimal coupling part of the action induced by the spin of the object. This part is initially formulated in terms of the definite-parity pseudovector S_μ , as defined in [16, 19, 24]. Beyond these non-minimal couplings all of the previous terms in the action are similar to what is noted in [25], where the difference with the action in [33–35] was highlighted.

The non-minimal coupling part of the effective action involving the spin was constructed in [16], where the spin-induced non-minimal couplings to all orders in spin and linear in the curvature were derived to be:

$$L_{\text{NMC(R)}} = \sum_{n=1}^{\infty} \frac{(-1)^n}{(2n)!} \frac{C_{ES^{2n}}}{m^{2n-1}} D_{\mu_{2n}} \cdots D_{\mu_3} \frac{E_{\mu_1\mu_2}}{\sqrt{u^2}} S^{\mu_1} S^{\mu_2} \cdots S^{\mu_{2n-1}} S^{\mu_{2n}} \\ + \sum_{n=1}^{\infty} \frac{(-1)^n}{(2n+1)!} \frac{C_{BS^{2n+1}}}{m^{2n}} D_{\mu_{2n+1}} \cdots D_{\mu_3} \frac{B_{\mu_1\mu_2}}{\sqrt{u^2}} S^{\mu_1} S^{\mu_2} \cdots S^{\mu_{2n}} S^{\mu_{2n+1}}, \quad (2.4)$$

which involves new spin-induced Wilson coefficients, the electric and magnetic curvature components of definite parity, defined as

$$E_{\mu\nu} \equiv R_{\mu\alpha\nu\beta} u^\alpha u^\beta, \quad (2.5)$$

$$B_{\mu\nu} \equiv \frac{1}{2} \epsilon_{\alpha\beta\gamma\mu} R^{\alpha\beta}{}_{\delta\nu} u^\gamma u^\delta, \quad (2.6)$$

as well as their covariant derivatives, D_μ . Of the infinite series in eq. (2.4) only the first operator is required in this paper, corresponding to the spin-induced quadrupole that reads:

$$L_{ES^2} = -\frac{C_{ES^2}}{2m} \frac{E_{\mu\nu}}{\sqrt{u^2}} S^\mu S^\nu. \quad (2.7)$$

Up to missing generic symmetry and construction considerations, a closely related expression was used in [36], which conformed with the well-known LO spin-squared interaction from [37, 38].

There are no additional Feynman rules (such as worldline mass and spin couplings) required for the $\text{spin}_1\text{-spin}_2$ and $\text{spin}_1\text{-spin}_1$ interactions, which originate from the minimal-coupling part of the point-particle action, beyond those presented in [20, 25]. Thus, we

turn now to the Feynman rules required for this sector due to the interaction involving the spin-induced quadrupole, which go beyond the rules in previously computed lower-order spinning sectors [21]. All of the aforementioned Feynman rules can be obtained within the public `EFTofPNG` code [23] for a generic number of spatial dimensions d . The new relevant Feynman rules for this sector were obtained by further extending the `FeynRu1` module of the `EFTofPNG` code [23].

For the three-graviton coupling to the worldline spin-induced quadrupole, the new required Feynman rule is

$$\begin{aligned}
 \text{Diagram} &= -\frac{C_{ES^2}}{4m} \frac{1}{d-2} \int dt \left[dS^i S^j \left(2\sigma_{ik} (\partial_j \phi \partial_k \phi + \phi \partial_j \partial_k \phi) + \phi \partial_k \phi (2\partial_i \sigma_{jk} - \partial_k \sigma_{ij}) \right) \right. \\
 &\quad \left. - S^2 \left(2\sigma_{ij} (\partial_i \phi \partial_j \phi + d\phi \partial_i \partial_j \phi) + d\phi \partial_i \phi (2\partial_j \sigma_{ij} - \partial_i \sigma_{jj}) \right) \right], \tag{2.8}
 \end{aligned}$$

while there is also a new Feynman rule for the four-graviton coupling to the worldline spin-induced quadrupole, given by

$$\begin{aligned}
 \text{Diagram} &= \frac{C_{ES^2}}{12m} \frac{d^2}{(d-2)^3} \int dt \left[dS^i S^j \left(3\phi^2 \partial_i \phi \partial_j \phi + \phi^3 \partial_i \partial_j \phi \right) \right. \\
 &\quad \left. - S^2 \left(3\phi^2 (\partial_i \phi)^2 + d\phi^3 \partial_i \partial_i \phi \right) \right]. \tag{2.9}
 \end{aligned}$$

We remind the reader that these rules are already given in terms of the physical spatial components of the local Euclidean spin vector in the canonical gauge [16], and that all of the indices are in fact Euclidean.

2.1 Extending the EFT of a spinning particle

To complete the effective action at this order in PN accuracy in the spinning sectors [21, 25] including the current sector, we extend the non-minimal coupling part of the effective action of a spinning particle given in eq. (2.4). This extension contains operators that are quadratic in the curvature components and hence stand for tidal deformations of the extended compact object. Following similar symmetry considerations and the logic outlined in [16], we find that the new terms to quadratic order in spin are given by

$$\begin{aligned}
 L_{\text{NMC(R}^2)} &= C_{E^2} \frac{E_{\alpha\beta} E^{\alpha\beta}}{\sqrt{u^2}^3} + C_{B^2} \frac{B_{\alpha\beta} B^{\alpha\beta}}{\sqrt{u^2}^3} + \dots \\
 &\quad + C_{E^2 S^2} S^\mu S^\nu \frac{E_{\mu\alpha} E_\nu^\alpha}{\sqrt{u^2}^3} + C_{B^2 S^2} S^\mu S^\nu \frac{B_{\mu\alpha} B_\nu^\alpha}{\sqrt{u^2}^3} \\
 &\quad + C_{\nabla EBS} S^\mu \frac{D_\mu E_{\alpha\beta} B^{\alpha\beta}}{\sqrt{u^2}^3} + C_{E\nabla BS} S^\mu \frac{E_{\alpha\beta} D_\mu B^{\alpha\beta}}{\sqrt{u^2}^3}
 \end{aligned}$$

$$+ C_{(\nabla E)^2 S^2} S^\mu S^\nu \frac{D_\mu E_{\alpha\beta} D_\nu E^{\alpha\beta}}{\sqrt{u^2}^3} + C_{(\nabla B)^2 S^2} S^\mu S^\nu \frac{D_\mu B_{\alpha\beta} D_\nu B^{\alpha\beta}}{\sqrt{u^2}^3} + \dots \quad (2.10)$$

These terms involve new tidal Wilson coefficients (that in contrast with eq. (2.4) are defined here to absorb all numerical and mass factors).

In the first line of eq. (2.10) we have written the leading mass-induced quadrupolar tidal deformations, which are known to enter at the 5PN order [15], and have suppressed higher-order mass-induced tidal operators, which can be found in [39]. We have additionally shown the adiabatic tidal operators which involve the spin up to quadratic order. From dimensional analysis and power-counting considerations (as explained in [15, 16]), one can infer that the terms in the second line of eq. (2.10) enter at the 5PN order, while the terms on the third and fourth lines of eq. (2.10) enter only at the 6.5PN and 7PN orders, respectively.

Therefore at the 5PN order considered in this work there are two new operators which are quadratic in the spin and quadratic in the curvature. However, the leading contribution from these operators at the 5PN order shows up in the two-graviton exchange topology at order G^2 (see e.g. figure 2(a) in [25]), and is therefore not relevant in the current paper, but rather will be addressed in a subsequent publication. Notice that interestingly if this expansion that is quadratic in the curvature is continued to higher orders in spin as in [26], only spin orders $l = 0, 2, 4$ that relate to bosons of quantum spin $s = 0, 1, 2$ enter at leading order. Spin orders that correspond to fermions and quantum spin $s > 2$ all require additional covariant derivatives and enter at higher orders.

3 Perturbative expansion of quadratic-in-spin interactions

In this paper we evaluate the contribution to the N³LO sector that is quadratic in the spins, and originates from Feynman graphs at order G^4 in the diagrammatic expansion of the two-particle effective action in eq. (2.1). A comprehensive analysis of the generic topologies at order G^4 in the EFT framework was presented in the recent work [25]. Using the terminology defined in that work, these topologies are shown in figure 1, classified according to their self-interaction vertices and the corresponding loop order in the worldline picture [25]. As in [25], it is only the graphs that are at three-loop order in the worldline picture that genuinely represent a higher level of complexity in the N³LO spinning sectors. These graphs have topologies (d), (f), or (g), as depicted in figure 1 (see also figure 12 in [15]).

As of the two-loop order we also have higher-rank topologies, which means that more than a single basic integral of n -loop form, as specified in [25], is required to express integrals of that topology. In general, a rank- r topology requires a combination of r of the basic n -loop integrals (at order G^{n+1}). In this sector at order G^4 we have four higher-rank topologies: Topology (e8) is a rank-two topology, whereas topologies (f5), (g4), and (g5), are rank-three topologies [25]. In contrast to the rank-one topologies, which easily boil down to one-loop computations, the higher-rank topologies require considerable processing mainly by means of integration-by-parts (IBP) [40].

We proceed to the construction of the Feynman graphs that contribute to this sector. We recall that the spinning sector is more complicated than the non-spinning sector, because all possible topologies are realized at each order in G , even when the KK field decomposition is used [28, 30, 31], in contrast to the non-spinning sector, where in particular at $N^n\text{LO}$ for odd n , n -loop graphs are absent, as can be seen in table 1. As we noted in section 2 this sector contains three types of interactions of two distinct origins: There are the $\text{spin}_1\text{-spin}_2$ and $\text{spin}_1\text{-spin}_1$ interactions, which originate from the minimal coupling part of the action of a spinning particle in eq. (2.3), and the interaction that involves the spin-induced quadrupole, which originates from the non-minimal coupling part of the action.

Graphs with the first two types of interaction are readily constructed as subsets of the corresponding graphs in the $N^3\text{LO}$ spin-orbit sector [25] by replacing in the graphs of the latter some of the worldline mass couplings to the gravito-magnetic vector with its leading linear spin couplings. The presence of two spin couplings among the worldline insertions leads to fewer unique graphs than in the $N^3\text{LO}$ spin-orbit sector, but still more than were present in the non-spinning sector. Graphs with the third type of interaction can similarly be obtained as a subset of the non-spinning $N^3\text{LO}$ sector [41, 42] by replacing some of the worldline mass couplings to the scalar graviton with its leading spin-quadrupole coupling, or by adding a scalar graviton exchange to the few graphs at order G^3 that can be made static as a result (we remind the reader that this even-parity sector is static at order G^4).

Therefore, as no three-loop graphs enter at this order in the non-spinning case when the KK field decomposition is used, there are in fact no three-loop graphs with the spin-induced quadrupole which contribute to the $N^3\text{LO}$ quadratic-in-spin sector; The only contribution to this sector dependent on the spin-induced quadrupole comes from graphs below three-loop order in the worldline picture, as can be seen in figure 6. Note that this is exactly what happens in the NLO spin-squared sector [16] due to the absence of one-loop graphs at the NLO non-spinning sector with the KK fields [30]. Altogether, this reasoning provided a complete crosscheck for the automated generation of the Feynman graphs using the **FeynGen** module of the **EFTofPNG** public code [23], which was extended to handle this sector. The resulting graphs are drawn in figures 2–6 below (using JaxoDraw [43, 44] based on [45]).

There are in total 163 distinct graphs in this sector. Of these 52 are three-loop graphs with $\text{spin}_1\text{-spin}_2$ and $\text{spin}_1\text{-spin}_1$ interactions, as shown in figures 3 and 5, respectively. There are 31 higher-rank graphs to evaluate. Of these 12 are rank-two and 19 are rank-three. The evaluation of the graphs was carried out using the upgrade to the publicly available **EFTofPNG** code which was described in [25], where the higher-rank graphs are reduced using projection [46–48] and IBP [49] methods. Due to the additional spin with respect to the spin-orbit sector further projection of the numerators of the integrands was required. Further, more integrals show up in this sector compared to the corresponding spin-orbit one.

In the ancillary files to this publication we list the values of each of the Feynman graphs, both in PDF form and in machine-readable form. We recall that all of the graphs in figures 2–6 should be accompanied by their ‘mirror’ graphs, in which worldline labels are exchanged, namely $1 \leftrightarrow 2$. We note that for the spin-squared interactions in figures 4–6 we

present the value for the graph with the spins on worldline “1”, while for the $\text{spin}_1\text{-spin}_2$ interaction in figures 2-3 we present the value for the graph with higher power of m_1 . Two independent implementations of the framework outlined thus far were carried out in the present work in order to crosscheck and verify all the new results we present.

Similar features to those which were noted in [25] are observed in this sector, with the new ones (which did not appear below N^3LO) similarly originating uniquely from three-loop topologies in the worldline picture. Let us enumerate the notable features encountered:

- 1. Zeros.** There are 15 graphs that vanish, 13 of which have topologies (c1) and (e4): these vanish due to contact interaction terms, as discussed in [25]. In addition, the graphs 4(e8.1), 4(e8.2) vanish, which was expected since these factorizable graphs contain the vanishing graph in figure 6(c1) in the N^2LO spin-squared sector [21] as a subgraph.
- 2. Riemann zeta values.** There are 7 graphs of the rank-three topologies (f5), (g4), (g5), that give rise to terms with $\zeta(2) \equiv \pi^2/6$, which occur as explained in [25].
- 3. Divergences and logarithms.** There are 36 graphs, which make up the majority of the three-loop graphs, that give rise to simple poles in the dimensional parameter $\epsilon \equiv d - 3$ in conjunction with logarithms in r/R_0 , where R_0 is some renormalization scale. They appear in virtually all three-loop topologies (except (d2), (f3), (g2)) and are discussed in [25].

We recall that the $\zeta(2)$ terms or the poles and accompanying logarithms originate independently from different basic integrals as explained in [25].

4 N^3LO gravitational quadratic-in-spin action at G^4

Summing all graphs at order G^4 , we obtain the following contribution to the N^3LO gravitational quadratic-in-spin action :

$$L_{\text{S}^2}^{\text{N}^3\text{LO}} = L_{\text{S}_1\text{S}_2}^{\text{N}^3\text{LO}} + L_{\text{S}_1^2}^{\text{N}^3\text{LO}} + L_{\text{C}_{1E\text{S}^2}\text{S}_1^2}^{\text{N}^3\text{LO}} + (1 \leftrightarrow 2), \quad (4.1)$$

with

$$L_{\text{S}_1\text{S}_2}^{\text{N}^3\text{LO}} = -\frac{G^4}{r^6} \frac{1}{m_1 m_2} \left[\vec{S}_1 \cdot \vec{S}_2 \left(5 m_1^4 m_2 + 63 m_1^3 m_2^2 \right) - \vec{S}_1 \cdot \vec{n} \vec{S}_2 \cdot \vec{n} \left(25 m_1^4 m_2 + 300 m_1^3 m_2^2 \right) \right], \quad (4.2)$$

$$L_{\text{S}_1^2}^{\text{N}^3\text{LO}} = \frac{G^4}{r^6} \frac{1}{m_1^2} \left[S_1^2 \left(\frac{1}{14} m_1^4 m_2 - \frac{73}{70} m_1^3 m_2^2 - m_1^2 m_2^3 \right) + (\vec{S}_1 \cdot \vec{n})^2 \left(\frac{23}{7} m_1^4 m_2 + \frac{2851}{70} m_1^3 m_2^2 + 31 m_1^2 m_2^3 \right) \right], \quad (4.3)$$

and

$$L_{C_{1ES^2}S_1^2}^{\text{N}^3\text{LO}} = -\frac{G^4}{r^6} \frac{C_{1ES^2}}{m_1^2} \left(S_1^2 - 3(\vec{S}_1 \cdot \vec{n})^2 \right) \left(\frac{23}{28} m_1^4 m_2 + \frac{341}{14} m_1^3 m_2^2 + 57 m_1^2 m_2^3 + 9 m_1 m_2^4 \right), \quad (4.4)$$

where $\vec{r} \equiv \vec{r}_1 - \vec{r}_2$ and $\vec{n} \equiv \vec{r}/r$.

Interestingly, in contrast to the situation in the N³LO spin-orbit sector [25], all divergent terms, logarithms, and factors of $\zeta(2)$ that appear in the individual graphs leading to eqs. (4.2) and (4.3) conspire to cancel out from the final result, which contains only finite rational terms. This is similar to the situation within analogous EFT derivations in the non-spinning sector, where all the poles in ϵ , logarithms, and Riemann zeta values conspire to cancel out in each of the NⁿLO sectors at G^{n+1} as known for $n \leq 5$ [50, 51]. We recall that both the non-spinning sector and the present one are static at the highest order in G , and have even parity with respect to the order of spin (see table 1). This contrasts with the odd-parity spin-orbit sector, where the analogous piece is non-static. It is curious then whether this occurrence carries over to all of the even-parity sectors in spin.

In any case, we know that the appearance and treatment of divergent terms and logarithms is related to the treatment of terms with higher-order time derivatives [13]. Since the appearance of higher-order time derivative terms is delayed by one order in the quadratic-in-spin sectors with respect to the spin-orbit sector, where it occurs already at the LO [52], it may have been expected that the related novel features that show up in the final N³LO spin-orbit result are absent from the final N³LO quadratic-in-spin result here.

5 Conclusions

In this paper we derived for the first time the complete static N³LO gravitational interactions that are quadratic in the spins in inspiralling compact binaries from Feynman diagrams with topologies at order G^4 within the framework of the EFT of spinning gravitating objects [16]. The derivation builds on the recent work in [25], in which an upgrade of the `EFTofPNG` public code [23] was carried out, with further extensions required for the present sector. The contribution we have calculated in this paper constitutes the most computationally challenging piece of the N³LO quadratic-in-spin sector in terms of integration, due to the three-loop level that is the highest loop level in this sector. This sector enters at the 5PN order for maximally-spinning compact objects, and complements the non-spinning sector at the same order, with relevant pieces in e.g. [50, 51] and [53].

This sector contains three types of interactions that originate from the two distinct parts of the effective action of a spinning particle, where in particular one interaction involves finite-size effects, which arise from the non-minimal coupling part of the point-particle action. Such effects distinguish between black holes and neutron stars, in contrast to the spin-orbit coupling or point-mass interactions. Further, at this PN order higher non-minimal coupling operators beyond linear in the curvature with spin need to be included for the first time. We have correspondingly extended the effective action formulated in [16] to include operators that are quadratic in the curvature, similar to [26] at the same

PN order. While we find such operators that are quadratic in spin, and that can enter at this PN order, they do not enter at this order in G^4 , and are thus left to a forthcoming publication.

The N³LO quadratic-in-spin interactions consist of a total of 163 unique graphs at order G^4 . Of these 52 are three-loop graphs, which arise uniquely from the interactions that originate from minimal spin coupling, and in which special features are observed, similar to the analogous sector in the spin-orbit interaction [25]. However, these features (including divergences, logarithms, and transcendental factors) conspire to cancel out in the final result, similar to what happens in the non-spinning sector within EFT derivations for $n \leq 5$ in the NⁿLO sectors at order G^{n+1} [51]. Nevertheless, the present sector is still considerably more challenging than the corresponding non-spinning sector. The evaluation of the remaining contributions up to order G^3 that are required to complete the N³LO quadratic-in-spin sector should be facilitated with our extended upgrade of the `EFTofPNG` code [23, 25], and this completion of the sector will be reported in forthcoming publications.

As previously noted, all of the sectors denoted with boldface entries in table 1, including the current sector, have been derived to date for all generic only within the framework of the EFT of gravitating spinning objects [16, 23–25]. Clearly, independent crosschecks of these precision results are essential, and thus overlapping studies, possibly with further modern amplitudes methods as in [54–58], are very welcome.

Acknowledgments

ML receives funding from the European Union’s Horizon 2020 research and innovation programme under the Marie Skłodowska Curie grant agreements No. 847523 and No. 764850, and from the Carlsberg Foundation. ML has also been supported by the European Union’s Horizon 2020 Framework Programme FP8/2014-2020 “preQFT” starting grant No. 639729. ML is grateful to Freddy Cachazo for the warm hospitality at Perimeter Institute where the final stages of this work were carried out. AJM and MvH are both supported by an ERC starting grant No. 757978 and a grant from the Villum Fonden No. 15369. AJM is also supported by a Carlsberg Postdoctoral Fellowship (CF18-0641). MvH is also supported by the European Union’s Horizon 2020 research and innovation programme under grant agreement No. 793151.

References

- [1] LIGO, VIRGO collaboration, B. P. Abbott et al., *Observation of Gravitational Waves from a Binary Black Hole Merger*, *Phys. Rev. Lett.* **116** (2016) 061102 [1602.03837].
- [2] “LIGO webpage.” <http://www.ligo.caltech.edu>.
- [3] “Virgo webpage.” <http://www.virgo-gw.eu>.
- [4] LIGO SCIENTIFIC, VIRGO collaboration, B. P. Abbott et al., *GWTC-1: A Gravitational-Wave Transient Catalog of Compact Binary Mergers Observed by LIGO and Virgo during the First and Second Observing Runs*, *Phys. Rev.* **X9** (2019) 031040 [1811.12907].

- [5] “KAGRA webpage.” <http://gwcenter.icrr.u-tokyo.ac.jp/en>.
- [6] “IndiGO webpage.” <http://www.gw-indigo.org>.
- [7] M. Punturo et al., *The Einstein Telescope: A third-generation gravitational wave observatory*, *Class. Quant. Grav.* **27** (2010) 194002.
- [8] KOREAN GRAVITATIONAL WAVE GROUP collaboration, H. J. Paik, H. M. Lee, K. Cho and J. Kim, *Gravitational-wave Detectors and a New Low-frequency Detector SOGRO*, *New Phys. Sae Mulli* **66** (2016) 272.
- [9] “ESA LISA webpage.” <http://sci.esa.int/lisa>.
- [10] TIANQIN collaboration, J. Luo et al., *TianQin: a space-borne gravitational wave detector*, *Class. Quant. Grav.* **33** (2016) 035010 [[1512.02076](#)].
- [11] A. Buonanno and T. Damour, *Effective one-body approach to general relativistic two-body dynamics*, *Phys.Rev.* **D59** (1999) 084006 [[gr-qc/9811091](#)].
- [12] T. Damour, *The General Relativistic Two Body Problem and the Effective One Body Formalism*, *Fundam. Theor. Phys.* **177** (2014) 111 [[1212.3169](#)].
- [13] L. Blanchet, *Gravitational Radiation from Post-Newtonian Sources and Inspiralling Compact Binaries*, *Living Rev. Rel.* **17** (2014) 2 [[1310.1528](#)].
- [14] W. D. Goldberger and I. Z. Rothstein, *An Effective field theory of gravity for extended objects*, *Phys.Rev.* **D73** (2006) 104029 [[hep-th/0409156](#)].
- [15] M. Levi, *Effective Field Theories of Post-Newtonian Gravity: A comprehensive review*, *Rept. Prog. Phys.* **83** (2020) 075901 [[1807.01699](#)].
- [16] M. Levi and J. Steinhoff, *Spinning gravitating objects in the effective field theory in the post-Newtonian scheme*, *JHEP* **09** (2015) 219 [[1501.04956](#)].
- [17] M. Levi, *Binary dynamics from spin1-spin2 coupling at fourth post-Newtonian order*, *Phys.Rev.* **D85** (2012) 064043 [[1107.4322](#)].
- [18] M. Levi and J. Steinhoff, *Equivalence of ADM Hamiltonian and Effective Field Theory approaches at next-to-next-to-leading order spin1-spin2 coupling of binary inspirals*, *JCAP* **1412** (2014) 003 [[1408.5762](#)].
- [19] M. Levi and J. Steinhoff, *Leading order finite size effects with spins for inspiralling compact binaries*, *JHEP* **06** (2015) 059 [[1410.2601](#)].
- [20] M. Levi and J. Steinhoff, *Next-to-next-to-leading order gravitational spin-orbit coupling via the effective field theory for spinning objects in the post-Newtonian scheme*, *JCAP* **1601** (2016) 011 [[1506.05056](#)].
- [21] M. Levi and J. Steinhoff, *Next-to-next-to-leading order gravitational spin-squared potential via the effective field theory for spinning objects in the post-Newtonian scheme*, *JCAP* **1601** (2016) 008 [[1506.05794](#)].
- [22] M. Levi and J. Steinhoff, *Complete conservative dynamics for inspiralling compact binaries with spins at fourth post-Newtonian order*, [1607.04252](#).
- [23] M. Levi and J. Steinhoff, *EFTofPNG: A package for high precision computation with the Effective Field Theory of Post-Newtonian Gravity*, *Class. Quant. Grav.* **34** (2017) 244001 [[1705.06309](#)].

- [24] M. Levi, S. Mougiakakos and M. Vieira, *Gravitational cubic-in-spin interaction at the next-to-leading post-Newtonian order*, *JHEP* **01** (2021) 036 [[1912.06276](#)].
- [25] M. Levi, A. J. McLeod and M. von Hippel, *NNNLO gravitational spin-orbit coupling at the quartic order in G* , *JHEP* **07** (2021) 115 [[2003.02827](#)].
- [26] M. Levi and F. Teng, *NLO gravitational quartic-in-spin interaction*, *JHEP* **01** (2021) 066 [[2008.12280](#)].
- [27] N. Arkani-Hamed, T.-C. Huang and Y.-t. Huang, *Scattering Amplitudes For All Masses and Spins*, [1709.04891](#).
- [28] M. Levi, *Next to Leading Order gravitational Spin1-Spin2 coupling with Kaluza-Klein reduction*, *Phys.Rev.* **D82** (2010) 064029 [[0802.1508](#)].
- [29] L. Blanchet, A. Buonanno and G. Faye, *Tail-induced spin-orbit effect in the gravitational radiation of compact binaries*, *Phys.Rev.* **D84** (2011) 064041 [[1104.5659](#)].
- [30] B. Kol and M. Smolkin, *Non-Relativistic Gravitation: From Newton to Einstein and Back*, *Class.Quant.Grav.* **25** (2008) 145011 [[0712.4116](#)].
- [31] B. Kol, M. Levi and M. Smolkin, *Comparing space+time decompositions in the post-Newtonian limit*, *Class.Quant.Grav.* **28** (2011) 145021 [[1011.6024](#)].
- [32] M. E. Peskin and D. V. Schroeder, *An Introduction to quantum field theory*. Addison-Wesley, Reading, USA, 1995.
- [33] A. J. Hanson and T. Regge, *The Relativistic Spherical Top*, *Annals Phys.* **87** (1974) 498.
- [34] I. Bailey and W. Israel, *Lagrangian Dynamics of Spinning Particles and Polarized Media in General Relativity*, *Commun.Math.Phys.* **42** (1975) 65.
- [35] R. A. Porto, *Post-Newtonian corrections to the motion of spinning bodies in NRGR*, *Phys.Rev.* **D73** (2006) 104031 [[gr-qc/0511061](#)].
- [36] R. A. Porto and I. Z. Rothstein, *Next to Leading Order Spin(1)Spin(1) Effects in the Motion of Inspiralling Compact Binaries*, *Phys.Rev.* **D78** (2008) 044013 [[0804.0260](#)].
- [37] B. Barker and R. O’Connell, *Gravitational Two-Body Problem with Arbitrary Masses, Spins, and Quadrupole Moments*, *Phys.Rev.* **D12** (1975) 329.
- [38] E. Poisson, *Gravitational waves from inspiraling compact binaries: The Quadrupole moment term*, *Phys.Rev.* **D57** (1998) 5287 [[gr-qc/9709032](#)].
- [39] D. Bini, T. Damour and G. Faye, *Effective action approach to higher-order relativistic tidal interactions in binary systems and their effective one body description*, *Phys.Rev.* **D85** (2012) 124034 [[1202.3565](#)].
- [40] V. A. Smirnov, *Feynman integral calculus*. Springer, Berlin, Germany, 2006.
- [41] M. Levi, *Binary dynamics at third post-Newtonian order via an effective field theory approach*, *unpublished* (2011) .
- [42] S. Foffa and R. Sturani, *Effective field theory calculation of conservative binary dynamics at third post-Newtonian order*, *Phys.Rev.* **D84** (2011) 044031 [[1104.1122](#)].
- [43] D. Binosi and L. Theussl, *JaxoDraw: A Graphical user interface for drawing Feynman diagrams*, *Comput. Phys. Commun.* **161** (2004) 76 [[hep-ph/0309015](#)].

- [44] D. Binosi, J. Collins, C. Kaufhold and L. Theussl, *JaxoDraw: A Graphical user interface for drawing Feynman diagrams. Version 2.0 release notes*, *Comput. Phys. Commun.* **180** (2009) 1709 [[0811.4113](#)].
- [45] J. A. M. Vermaseren, *Axodraw*, *Comput. Phys. Commun.* **83** (1994) 45.
- [46] R. Karplus and M. Neuman, *Non-Linear Interactions between Electromagnetic Fields*, *Phys. Rev.* **80** (1950) 380.
- [47] B. A. Kniehl, *Associated Production of Higgs and Z Bosons From Gluon Fusion in Hadron Collisions*, *Phys. Rev.* **D42** (1990) 2253.
- [48] T. Binoth, E. W. N. Glover, P. Marquard and J. J. van der Bij, *Two loop corrections to light by light scattering in supersymmetric QED*, *JHEP* **05** (2002) 060 [[hep-ph/0202266](#)].
- [49] S. Laporta, *High precision calculation of multiloop Feynman integrals by difference equations*, *Int. J. Mod. Phys.* **A15** (2000) 5087 [[hep-ph/0102033](#)].
- [50] S. Foffa, P. Mastrolia, R. Sturani, C. Sturm and W. J. Torres Bobadilla, *Static two-body potential at fifth post-Newtonian order*, *Phys. Rev. Lett.* **122** (2019) 241605 [[1902.10571](#)].
- [51] J. Blümlein, A. Maier and P. Marquard, *Five-Loop Static Contribution to the Gravitational Interaction Potential of Two Point Masses*, *Phys. Lett.* **B800** (2020) 135100 [[1902.11180](#)].
- [52] M. Levi, *Next to Leading Order gravitational Spin-Orbit coupling in an Effective Field Theory approach*, *Phys.Rev.* **D82** (2010) 104004 [[1006.4139](#)].
- [53] S. Foffa and R. Sturani, *Hereditary terms at next-to-leading order in two-body gravitational dynamics*, *Phys. Rev. D* **101** (2020) 064033 [[1907.02869](#)].
- [54] F. Cachazo and A. Guevara, *Leading Singularities and Classical Gravitational Scattering*, *JHEP* **02** (2020) 181 [[1705.10262](#)].
- [55] A. Guevara, *Holomorphic Classical Limit for Spin Effects in Gravitational and Electromagnetic Scattering*, *JHEP* **04** (2019) 033 [[1706.02314](#)].
- [56] C. Cheung, I. Z. Rothstein and M. P. Solon, *From Scattering Amplitudes to Classical Potentials in the Post-Minkowskian Expansion*, *Phys. Rev. Lett.* **121** (2018) 251101 [[1808.02489](#)].
- [57] Z. Bern, C. Cheung, R. Roiban, C.-H. Shen, M. P. Solon and M. Zeng, *Scattering Amplitudes and the Conservative Hamiltonian for Binary Systems at Third Post-Minkowskian Order*, *Phys. Rev. Lett.* **122** (2019) 201603 [[1901.04424](#)].
- [58] Z. Bern, C. Cheung, R. Roiban, C.-H. Shen, M. P. Solon and M. Zeng, *Black Hole Binary Dynamics from the Double Copy and Effective Theory*, *JHEP* **10** (2019) 206 [[1908.01493](#)].

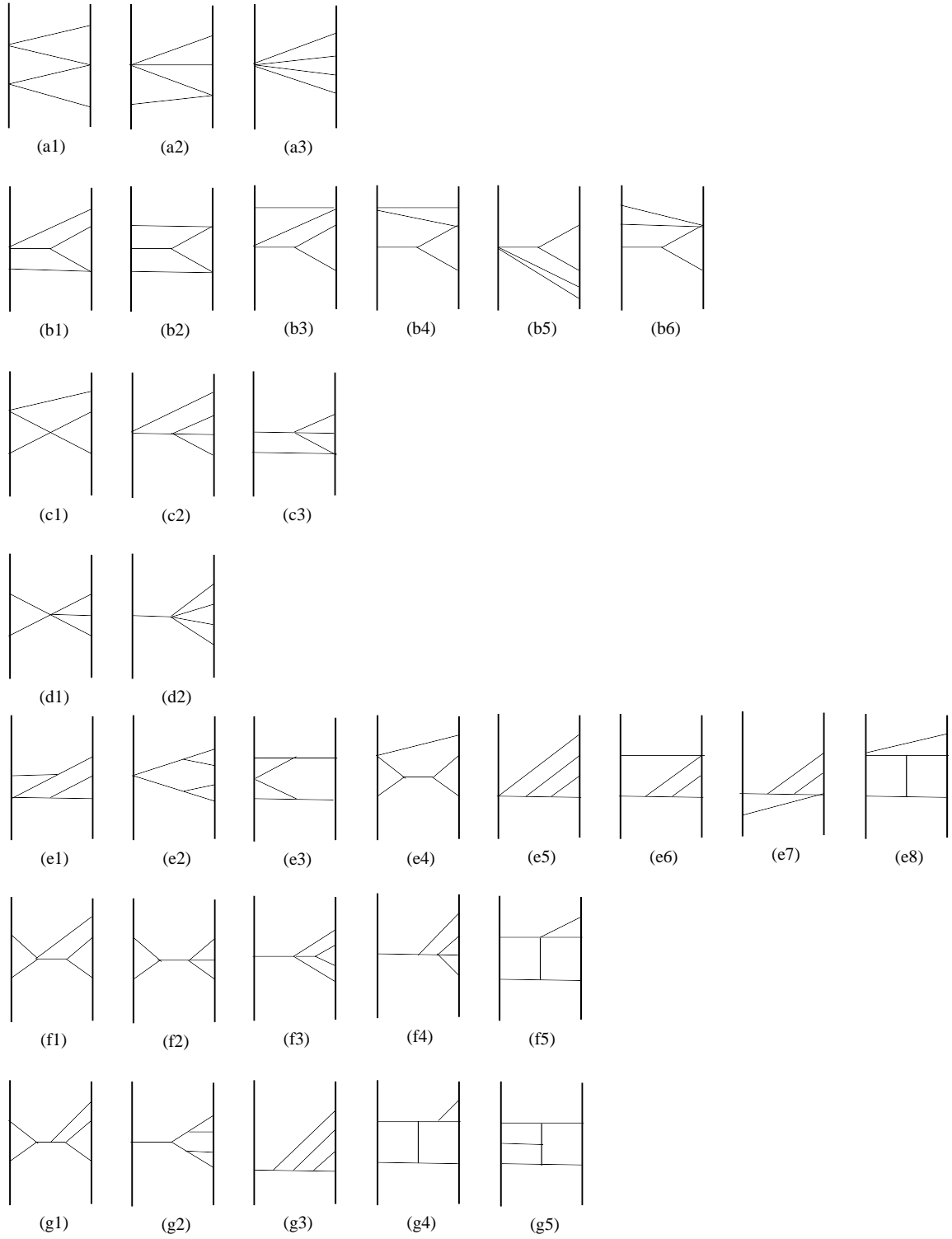


Figure 1. Graph topologies at order G^4 classified according to their internal bulk vertices and the corresponding loop order in the worldline picture [25]: (a) 0-loop; (b) One-loop; (c), (e) Two-loop; (d), (f), (g) Three-loop. Topology (e8) is a rank-two topology, whereas topologies (f5), (g4), and (g5), are rank-three topologies [25].

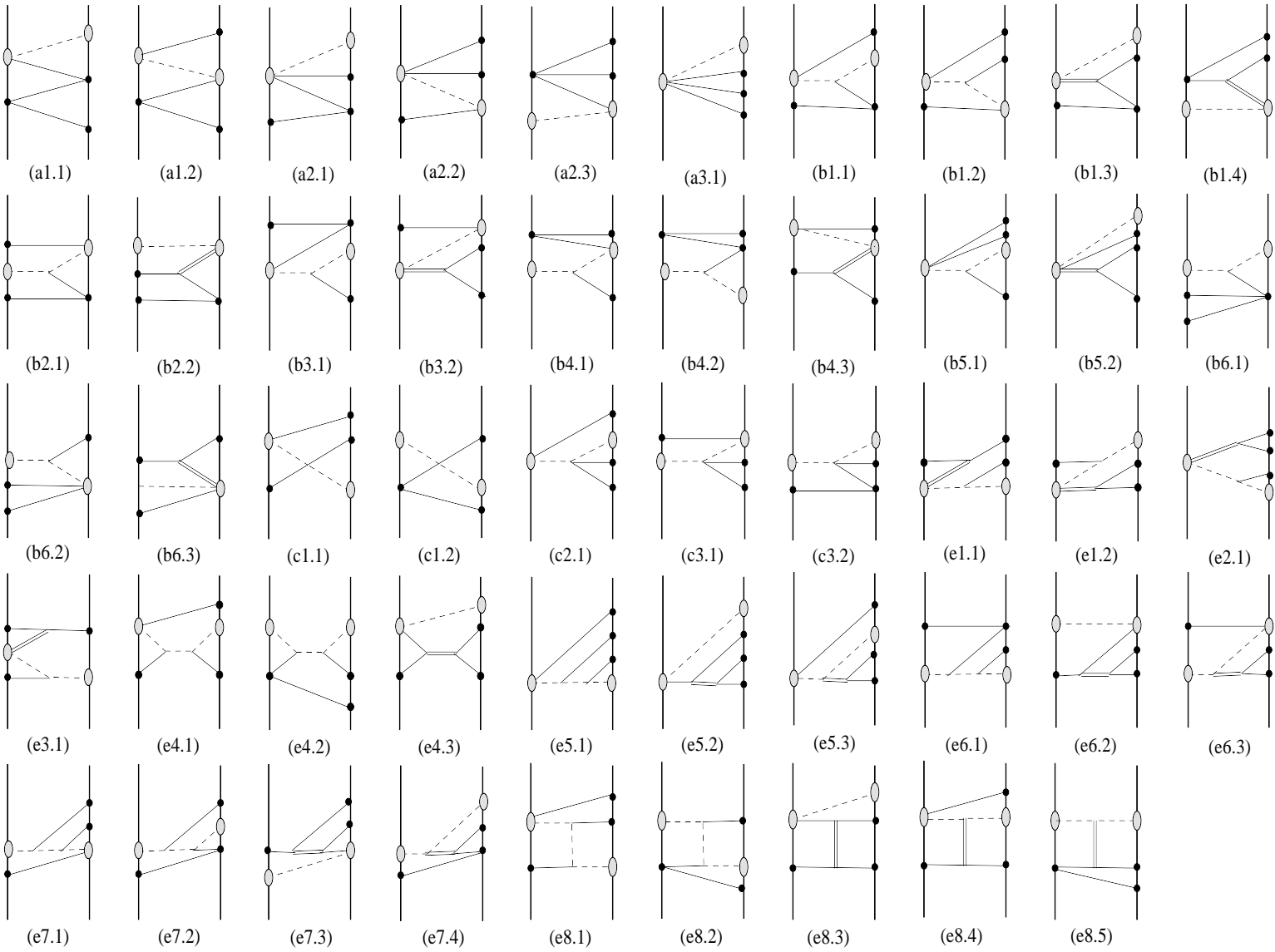


Figure 2. Feynman graphs below three-loop order in the worldline picture, which contribute to the $N^3\text{LO}$ spin-1-spin-2 static interaction at order G^4 . All of the graphs in this figure and the following ones should be accompanied by their ‘mirror’ graphs, in which worldline labels are exchanged, namely $1 \leftrightarrow 2$.

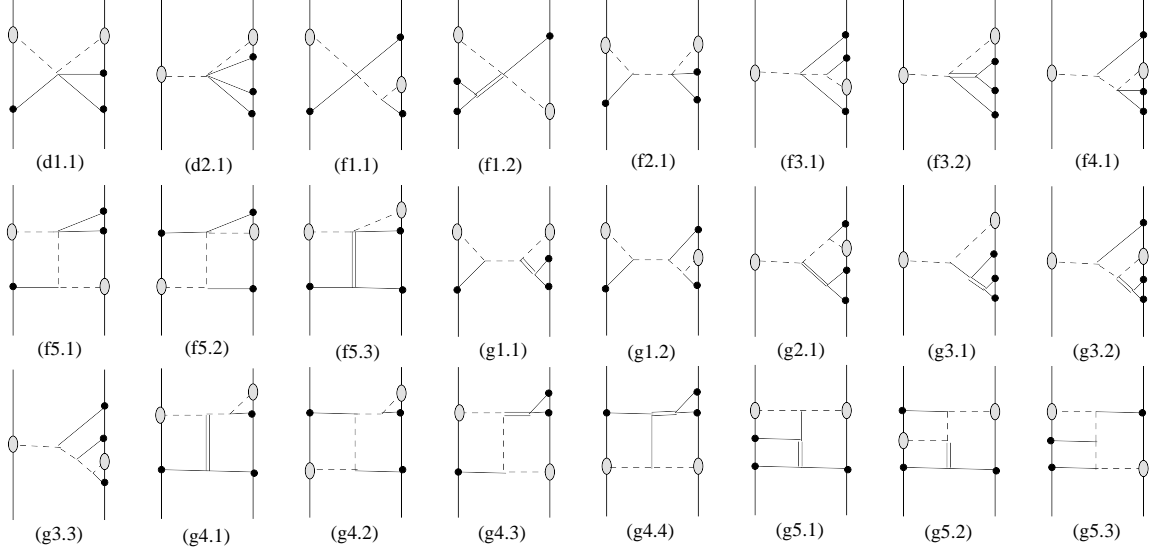


Figure 3. Feynman graphs at three-loop order in the worldline picture, which contribute to the $N^3\text{LO}$ $\text{spin}_1\text{-spin}_2$ static interaction at order G^4 .

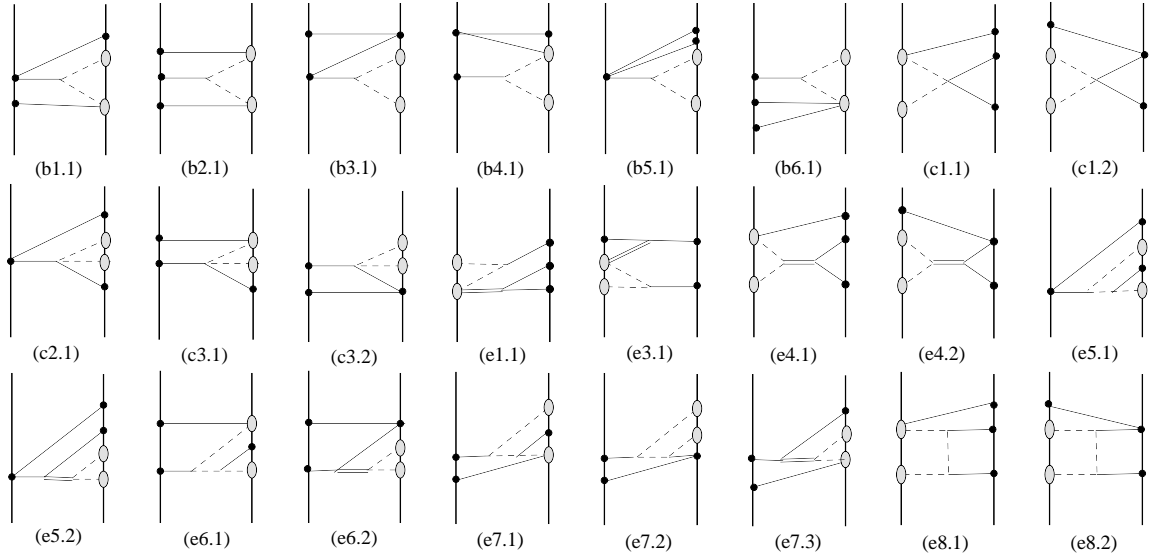


Figure 4. Feynman graphs below three-loop order in the worldline picture, which contribute to the $N^3\text{LO}$ $\text{spin}_1\text{-spin}_1$ static interaction at order G^4 .

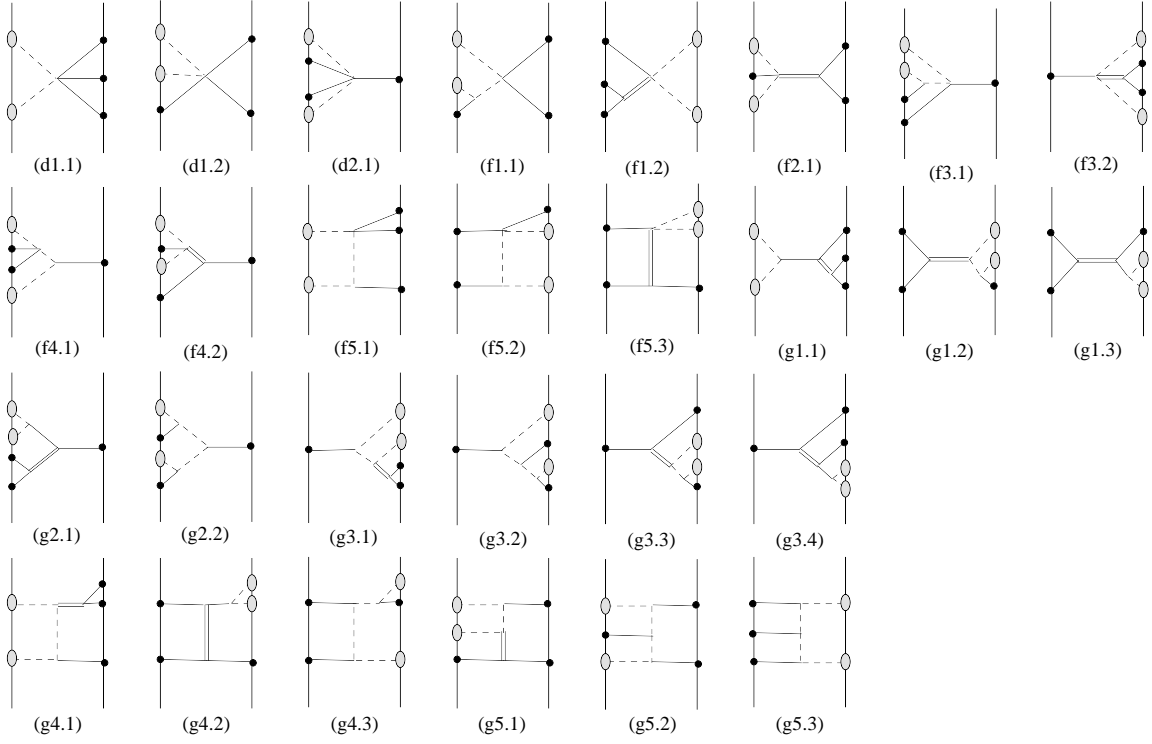


Figure 5. Feynman graphs at three-loop order in the worldline picture, which contribute to the $N^3\text{LO}$ $\text{spin}_1\text{-spin}_1$ static interaction at order G^4 .

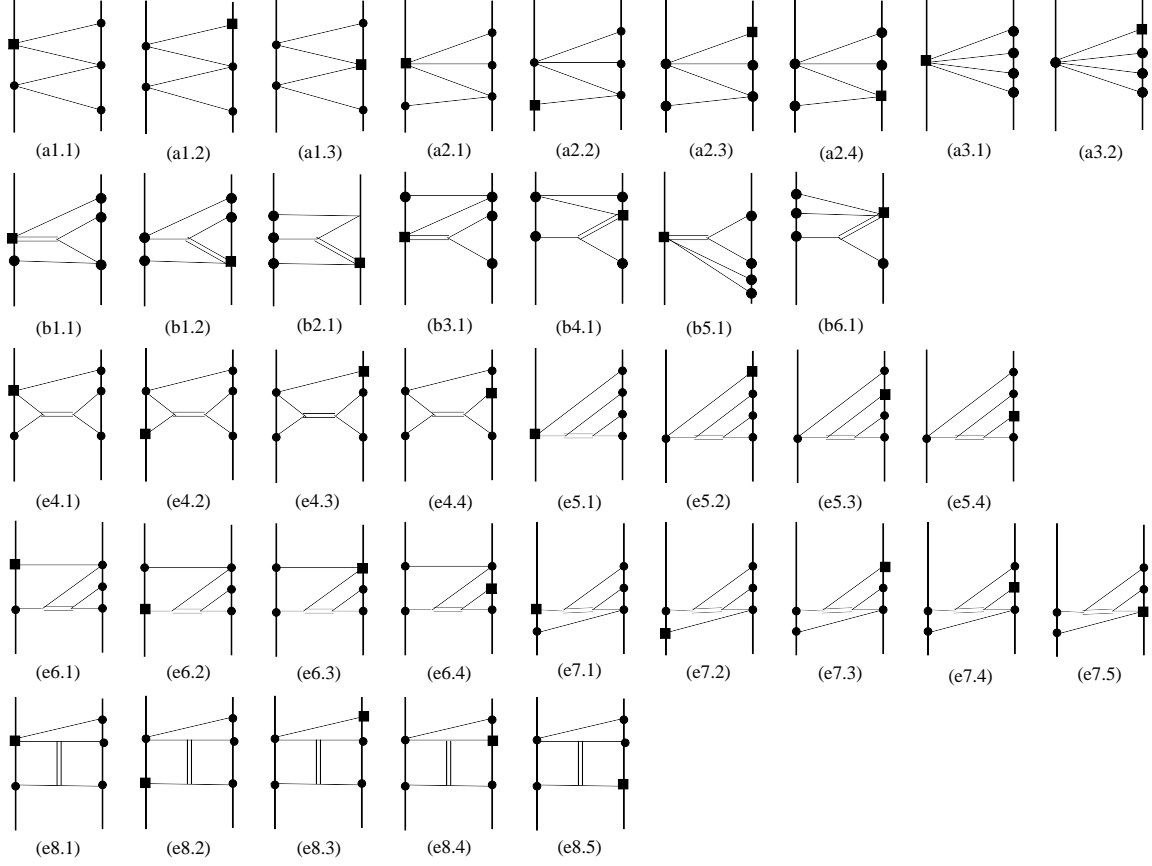


Figure 6. Feynman graphs below three-loop order dependent on the spin-induced quadrupole, which contribute to the $N^3\text{LO}$ quadratic-in-spin static interaction at order G^4 . This is the only contribution to the sector with the spin-induced quadrupole.